Ice-Tethered Profiler observations of the double-diffusive staircase in the Canada Basin thermocline

M.-L. Timmermans,[1] J. Toole,[1] R. Krishfield,[1] and P. Winsor[1]

Received 26 March 2008; revised 12 September 2008; accepted 2 October 2008; published 17 December 2008.

[1] Six Ice-Tethered Profilers (ITP), deployed in the central Canada Basin of the Arctic Ocean between 2004 and 2007, have provided detailed potential temperature and salinity measurements of a double-diffusive staircase at about 200–300 m depth. Individual layers in the staircase are of order 1 m in vertical height but appear to extend horizontally for hundreds of kilometers, with along-layer gradients of temperature and salinity tightly related. On the basis of laboratory-derived double-diffusive flux laws, estimated vertical heat fluxes through the staircase are in the range 0.05–0.3 W m^{-2}, only about one tenth of the estimated mean surface mixed layer heat flux to the sea ice. It is thus concluded that the vertical transport of heat from the Atlantic Water in the central basin is unlikely to have a significant impact to the Canada Basin ocean surface heat budget. Icebreaker conductivity-temperature-depth data from the Beaufort Gyre Freshwater Experiment show that the staircase is absent at the basin periphery. Turbulent mixing that presumably disrupts the staircase might drive greater flux from the Atlantic Water at the basin boundaries and possibly dominate the regionally averaged heat flux.

Citation: Timmermans, M.-L., J. Toole, R. Krishfield, and P. Winsor (2008), Ice-Tethered Profiler observations of the double-diffusive staircase in the Canada Basin thermocline, *J. Geophys. Res.*, *113*, C00A02, doi:10.1029/2008JC004829.

1. Introduction

[2] Warm and salty water enters the Arctic Ocean from the North Atlantic and subducts beneath the relatively cold and fresh surface waters to occupy a layer between about 250 and 800 m in the Canada Basin. It has long been noted that the heat contained in this Atlantic Water (AW) layer, if somehow transported vertically to the surface, is sufficient to completely melt the Arctic sea ice cover [e.g., *Rudels et al.*, 2004]. The large vertical salinity (and hence density) gradient above the AW in the Canada Basin inhibits the upward heat flux there. One of the most significant contemporary changes to occur in the Arctic Ocean has been a warming of the AW layer. Maximum temperatures of these waters are more than 1°C warmer since the 1990s compared to 1950–1989 [*Shimada et al.*, 2004; *Morison et al.*, 2000; *Serreze et al.*, 2000]. However, the impact to the sea ice cover of this AW heat content increase is only significant where it is energetically possible to transport this heat to the surface mixed layer. We focus here on estimating the vertical transport of heat from the AW. Well-mixed layers of uniform temperature and salinity have been observed at the upper boundary of the AW in the Canada Basin [*Neal et al.*, 1969; *Neshyba et al.*, 1971, 1972; *Neal and Neshyba*, 1973; *Perkin and Lewis*, 1984; *Padman and Dillon*, 1987, 1988, 1989]. This staircase structure is believed to be maintained by double-diffusive convection that can occur when colder, fresher water lies above warmer, salty water. By this mechanism, heat from the AW is transported upward across the diffusive interfaces between the well-mixed layers in the staircase.

[3] *Padman and Dillon* [1987, 1988, 1989] used microstructure measurements of temperature, conductivity and velocity shear (taken during the Arctic Internal Wave Experiment (AIWEX) in March–April 1985 (Figure 1)) to investigate the staircase structure in the central Canada Basin. Their 1987 paper found the staircase to be most clearly defined between 320 and 430 m depth, with 1 to 2 m thick homogeneous layers separated by high-gradient interfaces several centimeters thick across which the potential temperature jumps were $\delta\theta \approx 0.004 \rightarrow 0.012$°C. *Padman and Dillon* [1987, 1989] showed that the properties of the Canada Basin staircase were consistent with analytical and laboratory studies of double-diffusive convection, and estimated vertical heat fluxes associated with diffusive mixing to be in the range $0.02 \rightarrow 0.1$ W m^{-2}.

[4] Here we present temperature and salinity measurements of the double-diffusive staircase from a series of Ice-Tethered Profilers (ITP) that operated over a substantial portion of the Canada Basin between 2004 and 2007. In the next section, we review the ITP instrumentation and observations, then proceed in section 3 to describe the present-day staircase characteristics and report heat flux estimates. In section 4, we discuss turbulent heat transport from the AW, and infer turbulent mixing at the boundaries of the

[1]Woods Hole Oceanographic Institution, Woods Hole, Massachusetts, USA.

0148-0227/08/2008JC004829

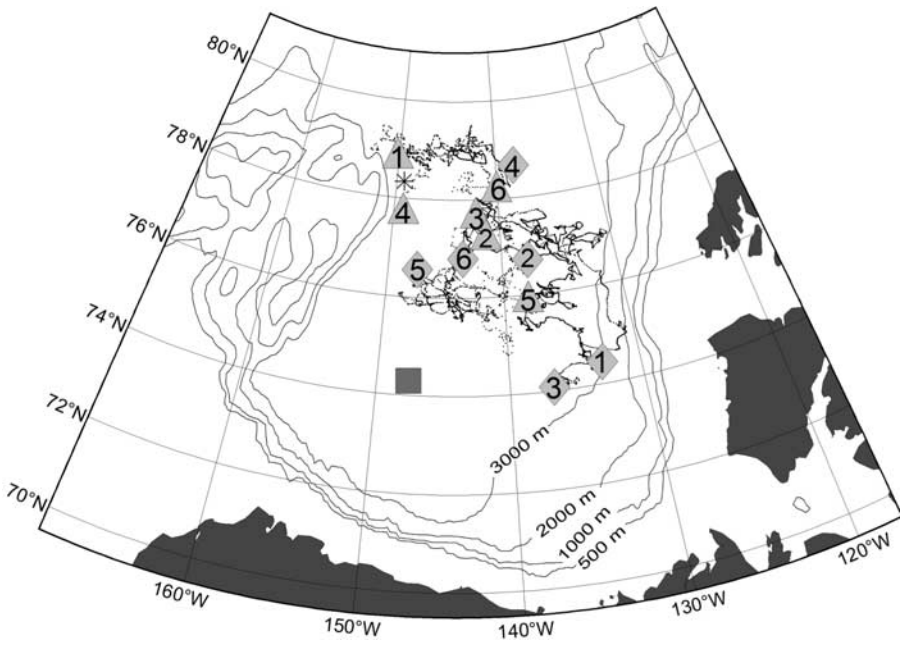

Figure 1. Map of ITP profile locations (each small dot denotes a profile, triangles denote the start of each ITP track, diamonds denote the end, and numbers denote the ITP system number) between August 2004 and October 2007. The square shows the 1985 Arctic Internal Wave Experiment region [*Padman and Dillon*, 1987, 1988, 1989], and the asterisk denotes the position of a microstructure profile from the August 2005 expedition of the Swedish icebreaker *Oden*.

Canada Basin where the well-formed staircase is not observed. The results are summarized in a concluding section.

2. Observations

[5] The ITP is an automated profiling conductivity-temperature-depth (CTD) probe that returns frequent (two or more profiles per day) high vertical resolution measurements of upper ocean temperature and salinity beneath sea ice during all seasons. The ITP is deployed through a 25 cm diameter hole drilled in perennial ice that is typically between 2 and 4 m thick. The system includes a profiling vehicle that cycles vertically along a weighted tether from just below the supporting ice floe to typically 760 m depth on a preprogrammed sampling schedule. The CTD on the ITP samples at 1 Hz and the vehicle profiles at a speed of about 25 cm s^{-1}, so that the raw data have a vertical resolution of around 25 cm. Communication between the profiler and surface controller is by means of an inductive modem. Full-resolution ITP sensor data are transmitted from the underwater profiler to the surface buoy via the modem and relayed to shore via the Iridium Satellite system. The ITP data are processed immediately upon reception and preliminary products are made directly available on the web (www.whoi.edu/itp). Technical details of the ITP system are given by *Krishfield et al.* [2006, 2008], and at www.whoi.edu/itp.

[6] The observations presented here are collected from six ITPs that drifted with the multi-year ice pack in the Canada Basin (the anticyclonic Beaufort Gyre). Typical ice drift speeds are around 10–20 cm s^{-1}, an order of magnitude larger than typical upper ocean current speeds in the Canada Basin. Differences observed in sequential ITP profiles are therefore interpreted here as spatial as opposed to temporal changes. Between August 2004 and October 2007, these six ITPs (Table 1) returned over 6400 profiles of temperature and salinity from 7–10 m down to 760 m depth (other ITPs are presently operating in the Canada Basin; see www.whoi.edu/itp). These ITP CTD data were corrected for sensor response errors following procedures detailed by *Johnson et al.* [2007]. The conductivity data were calibrated relative to recent ship observations from the region, and then edited to remove profile segments where the CTD sensor was obviously fouled. The conductivity calibration involved the derivation of profile-dependent multiplicative adjustments to match ITP potential conductivities on the 0.4 and 0.5°C potential temperature surfaces (below the AW core) to spatially varying reference fields on the basis of the shipboard data. The resulting ITP salinity data match the ship data to better than 0.005. On the basis of postdeployment calibration of two ITPs that were recovered (ITPs 1 and 4), we estimate temperature and pressure sensor accuracies to be ± 0.001°C and ±1 dbar, respectively. We use the final 1 Hz time series data (available via the ITP web site) for the present analysis as the 1 dbar bin-averaged data (also produced and available as above) do not adequately resolve the thermohaline staircase stratification.

3. Double-Diffusive Staircase

3.1. Regional Hydrography

[7] The double-diffusive convection at the upper boundary of the AW taps the potential energy associated with the unstably stratified temperature field, the AW having a maximum temperature around 350 m depth (Figure 2). The AW core waters are warmest near the AW inflow to the Canada Basin in the northwestern sector of the basin (Figure 3a) with no discernable seasonal variability over the

Table 1. Tabulation of Recent ITP Deployments in the Canada Basin[a]

ITP Number	Start Position	Start Date	End Date	Profiles per Day	Total Profiles
1	78.9°N, 150.3°W	15 Aug 2005	8 Aug 2007	4	2043
2	77.2°N, 141.2°W	19 Aug 2004	28 Sep 2004	6	244
3	77.6°N, 142.2°W	23 Aug 2005	9 Sep 2006	4	1532
4	78.1°N, 149.0°W	3 Sep 2006	16 Aug 2007	2	698
5	75.9°N, 138.0°W	7 Sep 2006	7 Sep 2007	3	1095
6	77.9°N, 140.4°W	5 Sep 2006	9 Oct 2007	2	799

[a]A total of approximately 3200 CTD profiles from these systems were used in our analysis (only the up-going profiles). (See www.whoi.edu/itp for ITPs operating presently in the Canada Basin.)

measurement period. AW heat is advected eastward and southward into the basin interior by relatively warm/salty intrusions that propagate from the core of the inflowing AW (see, for example, *McLaughlin et al.* [2004]). Given the thermal expansion coefficient $\alpha = -\rho^{-1}\partial\rho/\partial\theta$ and the saline contraction coefficient $\beta = \rho^{-1}\partial\rho/\partial S$ (density ρ) (α and β are calculated using *McDougall*'s [1987] algorithms coded by *Morgan* [1994]), double diffusion can occur when the density ratio (based on vertical gradients of S and θ), $\overline{R_\rho} = \overline{\beta\partial S/\partial z}/\overline{\alpha\partial\theta/\partial z} > 1$, where the overbar denotes the mean over the thermocline. In the thermocline in the ITP survey region, $3 \lesssim \overline{R_\rho} \lesssim 6$, with a trend toward higher values from northwest to southeast across the basin (Figure 3b). Note that ITPs were deployed over the abyssal plain of the central Canada Basin to avoid collision with the continental slope; in section 4, we will use an additional ship-derived hydrographic data set to investigate regions of the basin near lateral boundaries.

3.2. Staircase Characteristics

[8] Double-diffusive staircase stratification is present over a significant area of the Canada Basin; all but a small fraction of the ITP profiles (Figure 1) indicate a staircase between about 200 and 300 m (The staircase is absent in less than 4% of ITP profiles. No staircase is observed at the outer edges of a warm core AW eddy where presumably it was disrupted by the associated high geostrophic shear. The staircase is also absent in several other profiles about eddy-like features, and in the easternmost region sampled by ITP 1 close to the 3000 m isobath.) The staircase consists of a series of sharp interfaces across which both θ and S increase with depth separated by 1 to 5 m thick well-mixed convective layers (Figure 2). We used a layer detection technique that is based on potential temperature gradients to characterize the staircase structure over many ITP profiles. Mixed layers were identified in the depth range of the staircase where finite difference estimates of $\partial\theta/\partial z$ were much less than $\overline{\partial\theta/\partial z}$. We deduced an appropriate threshold for layer detection of $\partial\theta/\partial z < 0.005°\text{C m}^{-1}$. Note that the tight $\theta - S$ relationship in the thermocline allows us to use potential temperature to identify layers. The potential temperature and salinity differences across interfaces are found to be $\delta\theta \approx 0.04°\text{C}$ and $\delta S \approx 0.014$. The present day staircase is about 100 m shallower than measured in Padman and Dillon's surveys before the recent warming and shoaling of the AW, and in general with larger mixed layer thicknesses and temperature differences between layers. Note however that there is some variability in the depth of the staircase throughout the area sampled by ITPs, with deeper staircase and AW temperature maximum (around 400 m) closer to the region of the AIWEX study (Figure 1). This depth variability may be due in part to temporal vertical excursions of the water column. We will show, however, that the staircase layers are tightly related in $\theta - S$ space over the survey region, indicating a predominantly spatial variability in staircase $\theta - S$ properties.

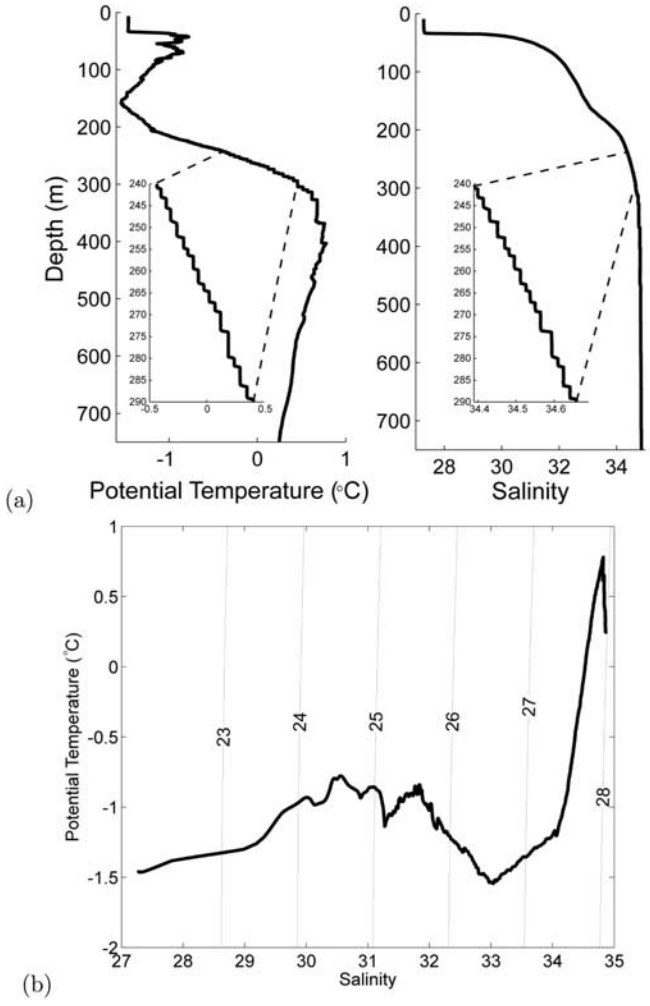

Figure 2. (a) Typical ITP profiles of potential temperature θ and salinity S in the Canada Basin (ITP 3, profile 1073, 19 May 2006, 138°W, 75°N). The expanded scales show the double-diffusive staircase. In these profiles, the Arctic surface mixed layer extends to about 40 m depth, with shelf-modified Pacific water from the Bering Strait immediately below. A strong thermocline denotes the boundary between the upper waters and the AW. Within the thermocline, temperature and salinity increase monotonically with depth, a necessary condition for double-diffusive layering. (b) The corresponding $\theta - S$ curve and lines of constant potential density anomaly (referenced to the surface).

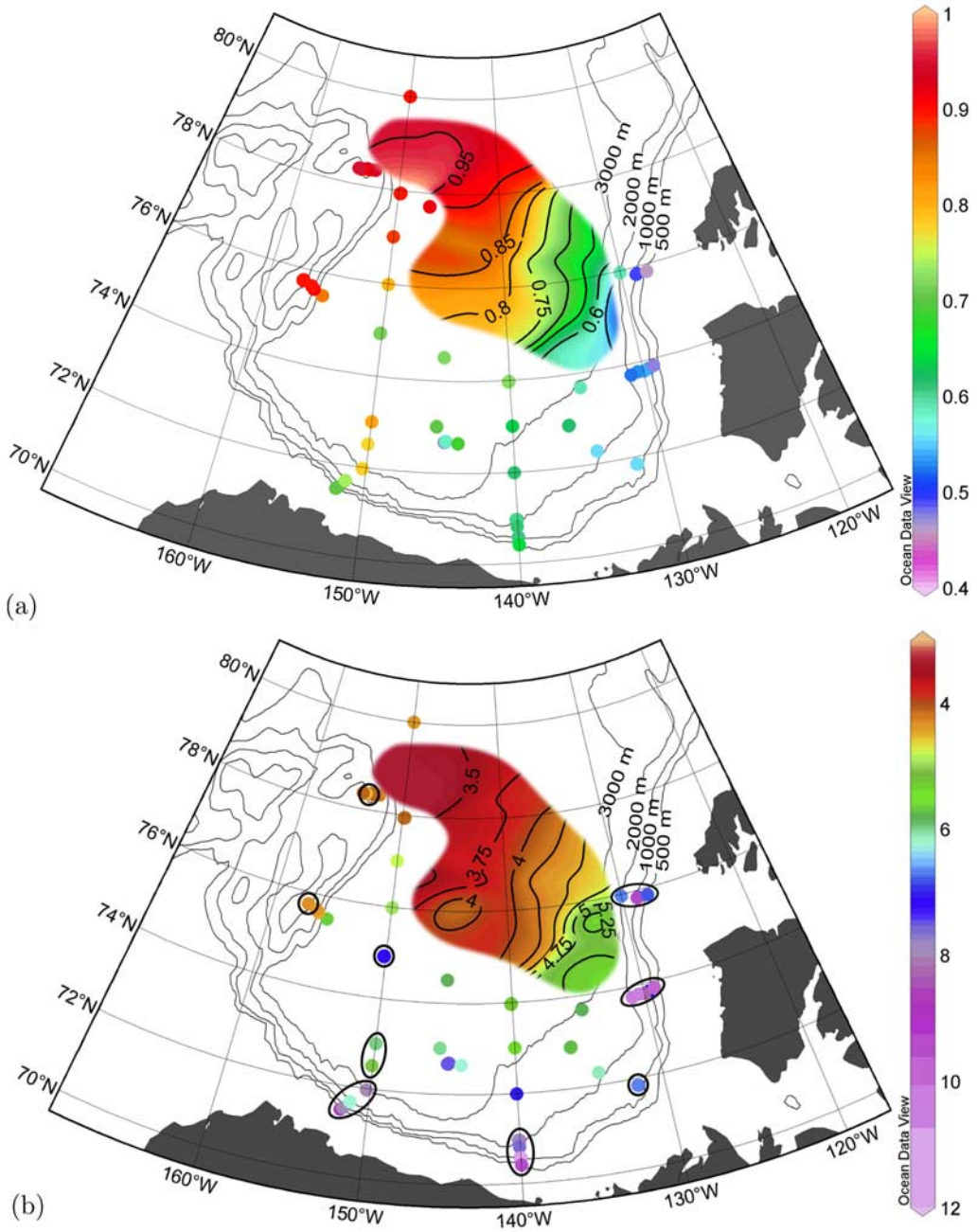

Figure 3. Atlantic Water (a) potential temperature (°C) maximum and (b) density ratio $\overline{R_\rho}$ averaged over the thermocline contoured from ITP measurements between August 2004 and October 2007. CTD stations from the Beaufort Gyre Observing System (data are available at www.whoi.edu/beaufortgyre/index.html) 2007 field program aboard the Canadian Coast Guard icebreaker *Louis S. St-Laurent* are shown as dots. Stations with no double-diffusive staircase are circled in Figure 3b.

[9] The stability of diffusive interfaces can be characterized in terms of the density ratio R_ρ between adjacent mixed layers, $R_\rho = (\beta\delta S)/(\alpha\delta\theta)$. *Padman and Dillon* [1987] calculated R_ρ values averaged over several steps, obtaining values ranging from about 4 to 6 from their 1985 observations. ITP profiles indicate values $2 \lesssim R_\rho \lesssim 7$ (Figure 4 with a spatial distribution as in Figure 3b), with no discernible depth dependence.

[10] We have identified a striking lateral coherence of individual mixed layers in the staircase by plotting points in $\theta - S$ space. Staircase mixed layer $\theta - S$ properties group along lines that cross isopycnals (Figure 5), indicating individual mixed layers are coherent across the entire basin (about 800 km) with aspect ratios on the order of 10^6. When normalized by β/α, the slope of the lines in $\theta - S$ space is remarkably constant (Figure 6); the inverse slope (lateral density ratio) is given by

$$R_{\rho x} = \frac{\beta S_x}{\alpha \theta_x} = -3.7 \pm 0.9, \tag{1}$$

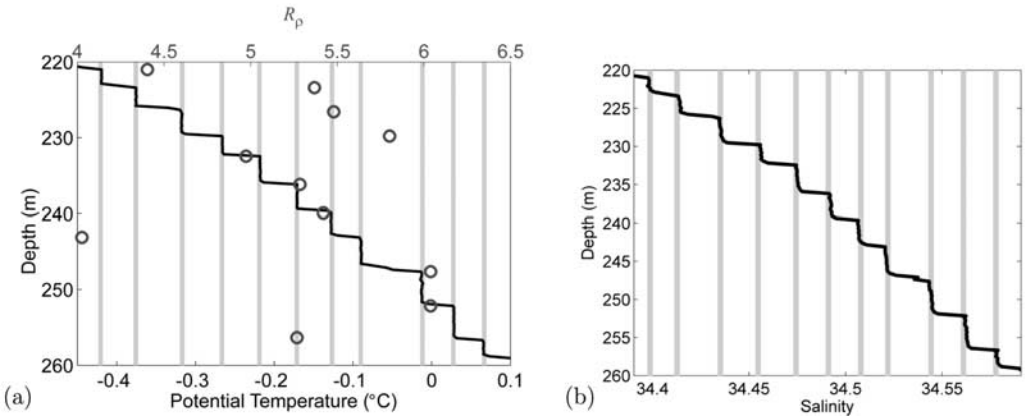

Figure 4. ITP profiles of (a) potential temperature and (b) salinity in the Canada Basin (ITP2, profile 185, 19 September 2004, 134°W, 77°N). The vertical gray bars indicate the results of a layer detection technique based on potential temperature gradients. The density ratio R_ρ for each step is also plotted (circles) in Figure 4a at the depth of each gradient region between layers.

where S_x and θ_x are the lateral changes in salinity and potential temperature for a given layer. Note that an analogous clustering in $\theta - S$ space was shown to occur for the salt fingering double-diffusive instability in the Caribbean Sheets and Layers Transects (CSALT) experiment [*Schmitt*, 1988; *Schmitt et al.*, 1987], where individual layers in a thermohaline staircase in the western tropical North Atlantic could be traced in $\theta - S$ space over more than 500 km.

[11] In (near) steady state, layer θ and S values are determined by a balance along the layer between lateral advective divergence and the vertical divergence of the double-diffusive heat and salt fluxes. If the vertical velocity is vertically uniform (or zero), then the horizontal divergence of velocity vanishes, by continuity, so the lateral advective divergence can be replaced by lateral advection. Hence the ratio,

$$R_{\rho x} = \frac{\beta \partial S/\partial x}{\alpha \partial \theta/\partial x} = \frac{\beta \partial q_s/\partial z}{\alpha \partial q_\theta/\partial z}, \tag{2}$$

where q_S (in m s^{-1}) and q_θ (in °C m^{-1} s^{-1}) are the fluxes of salt and temperature. In a manner similar to *McDougall* [1991] who considered layering in the salt-fingering case, an equation for the flux divergence ratio can be found by taking the vertical derivative of the flux ratio $R_f = (\beta\ q_S)/(\alpha q_\theta)$ as follows,

$$\frac{\beta \partial q_s/\partial z}{\alpha \partial q_\theta/\partial z} = R_f \left(1 - \frac{\alpha}{\beta} \frac{\partial(\beta/\alpha)}{\partial z} \frac{q_\theta}{\partial q_\theta/\partial z}\right) + \frac{dR_f}{dz} \frac{q_\theta}{\partial q_\theta/\partial z}. \tag{3}$$

Using (2) in (3) yields,

$$\frac{dR_f}{dz} + R_f \left(\frac{\partial q_\theta/\partial z}{q_\theta} - \frac{\alpha}{\beta} \frac{\partial(\beta/\alpha)}{\partial z}\right) - R_{\rho x} \frac{\partial q_\theta/\partial z}{q_\theta} = 0. \tag{4}$$

Assuming a flux ratio that is independent of depth (R_f depends on R_ρ, and, while there is a trend toward increasing R_ρ from west to east across the basin, R_ρ appears to be independent of depth.) (4) may be written as

$$R_{\rho x} = R_f \left(1 - \frac{\alpha}{\beta} \frac{\partial(\beta/\alpha)}{\partial z} \frac{q_\theta}{\partial q_\theta/\partial z}\right). \tag{5}$$

Experiments to measure the temperature and salinity of laboratory mixed layers as functions of time indicate that the ratio of vertical fluxes approaches a constant value $R_f \approx 0.15$ for $2 \leq R_\rho \leq 8$ [*Turner*, 1968]. Over the height of the staircase (about 100 m),

$$\frac{\alpha}{\beta} \frac{\partial(\beta/\alpha)}{\partial z} \approx 0.005 \text{ m}^{-1}.$$

Our calculations discussed in the next section indicate that the temperature flux changes very little over the depth of the staircase, thus a large-scale height (i.e., $q_\theta/(\partial q_\theta/\partial z) \gg 1$) is not unreasonable. For example, a scale height of about 5 km, together with the laboratory-based $R_f \approx 0.15$ could explain (1). It is also possible that other physical processes (*McDougall* [1991] cites migration of interfaces and vertical turbulent mixing in the case of salt fingers) may affect the lateral density ratio in thermohaline staircase layers.

3.3. Heat Fluxes

[12] Several laboratory experiments combined with theoretical analyses and best fits to oceanic cases have addressed the issue of heat fluxes across diffusive interfaces. A comprehensive review is given by *Kelley et al.* [2003]. Formulations have been derived to compute the vertical heat transport through a double-diffusive staircase as a function of the temperature difference across an interface between two adjacent mixed layers to the 4/3 power (“4/3 flux laws”). Hence, it is not necessary to know the thicknesses of interfaces between mixed layers in the staircase to determine fluxes, only the change in temperature $\delta\theta$ from one mixed layer to the next. On the basis of comparisons given by *Kelley et al.* [2003], we use arguably the most

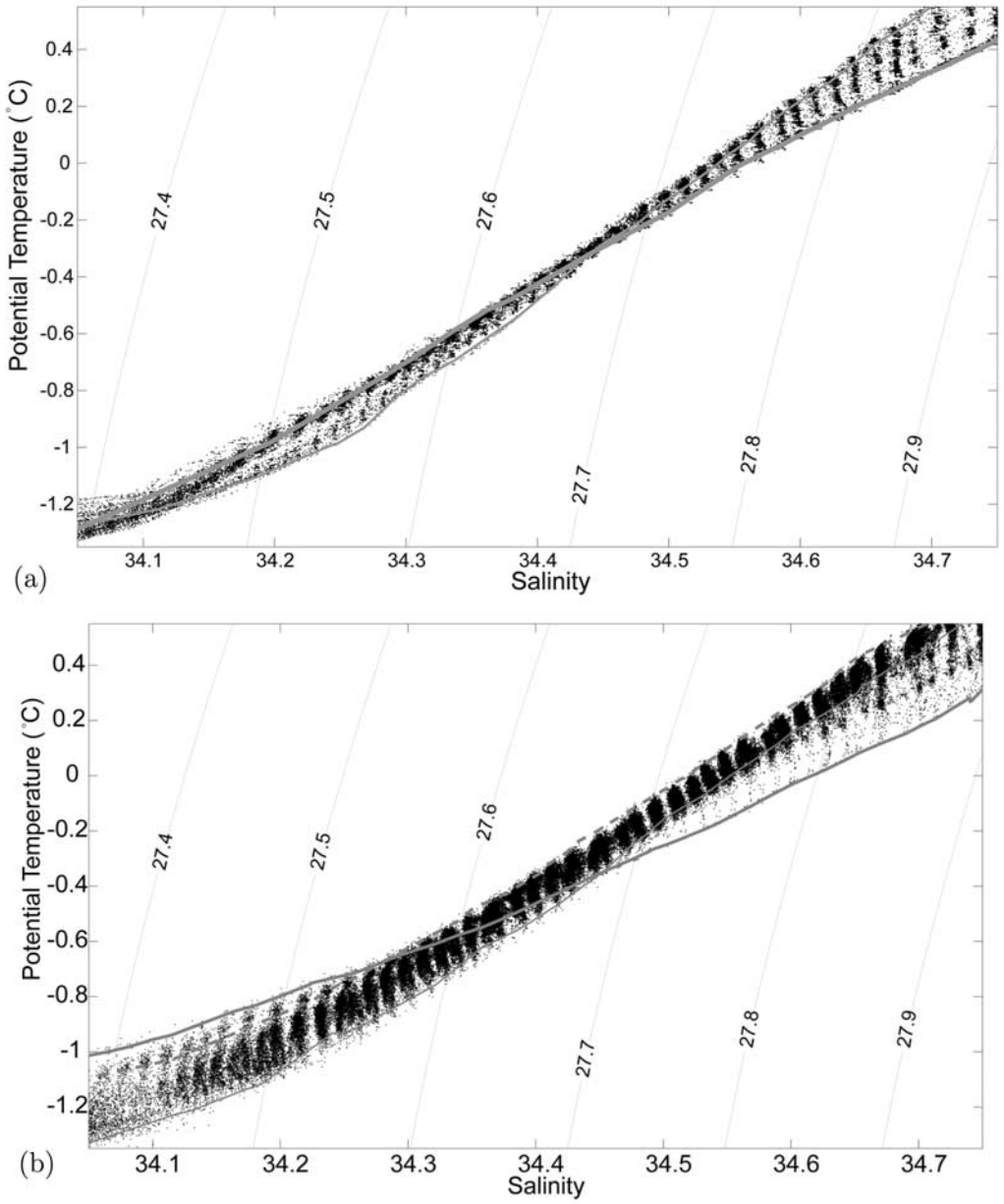

Figure 5. (a) $\theta - S$ values measured by ITP 2 between 200 m and 300 m depth. The westernmost (thin) and easternmost $\theta - S$ curves from the instrument drift track (a total east-west distance of about 180 km) are shown, as well as lines of constant potential density anomaly (referenced to the surface). This prototype instrument drifted east or southeast for the first three fourths of its abortive 40-day lifetime, then backtracked west. We observe no differences in the layer $\theta - S$ clustering between the eastward and westward legs. (b) Layer-averaged $\theta - S$ values measured by ITPs 1–6. Three $\theta - S$ curves from different regions of the basin show bounding water properties, where the curves are from 75°N, 132°W (thick); 79°N, 150°W (thin); and 76°N, 141°W (dashed). Staircase mixed layer properties tend to group along lines, indicating individual mixed layers are coherent for about 800 km across the basin and persist for several years.

appropriate formulation derived by *Kelley* [1990] to estimate double-diffusive fluxes through the Canada Basin staircase. The double-diffusive heat flux (in W m^{-2}) is given by *Kelley* [1990] as

$$F_H = 0.0032 e^{(4.8/R_\rho^{0.72})} \rho c_p \left(\frac{\alpha g \kappa}{Pr}\right)^{1/3} (\delta\theta)^{4/3}, \qquad (6)$$

where ρ is the density, c_p (in J kg^{-1} $°C^{-1}$) is the specific heat of the water, $Pr = \nu/\kappa$ is the Prandtl number, $\nu = 1.8 \times 10^{-6}$ m^2 s^{-1} is the kinematic viscosity, $\kappa = 1.4 \times 10^{-7}$ m^2 s^{-1} is the molecular diffusivity of heat, and $g = 9.8$ m s^{-2}. Using (6), we estimate the heat flux through each step in every ITP profile to be $F_H \approx 0.05 - 0.3$ W m^{-2} (Figure 7). As expected, heat fluxes are largest in the northwest, closest

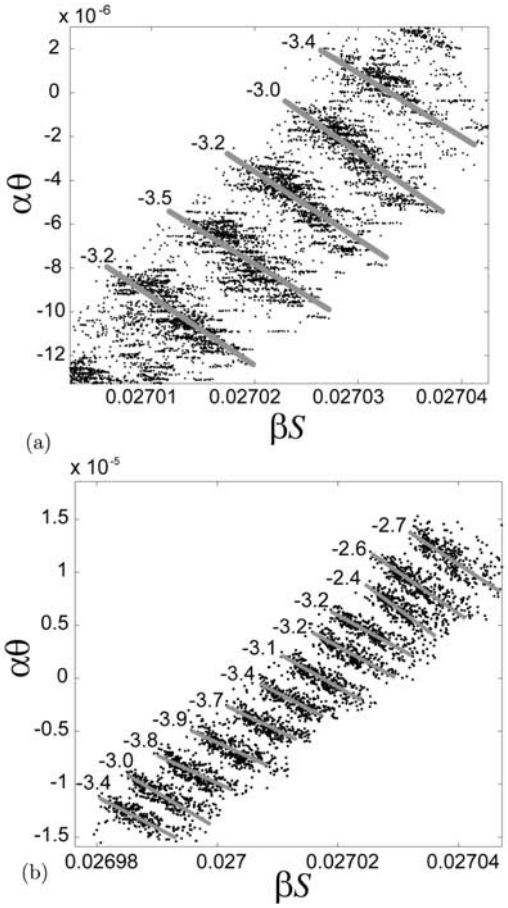

Figure 6. (a) ITP 2 and (b) ITP 5 $\theta - S$ values (normalized by β/α) through a portion of the staircase ($S \approx 34.4 \rightarrow 34.6$). The slope of lines formed by each mixed layer is approximately constant (lateral density ratios $R_{\rho x}$ are given).

to the inflowing AW core and lowest in the southeastern corner of the basin.

[13] *Padman and Dillon* [1987] used *Marmorino and Caldwell*'s [1976] double-diffusive heat flux parametrization given by

$$F_H = 0.0086 e^{(4.6 \exp\{-0.54(R_\rho - 1)\})} \rho c_p \left(\frac{\alpha g \kappa}{Pr}\right)^{1/3} (\delta\theta)^{4/3}, \quad (7)$$

to estimate heat fluxes through the Canada Basin staircase. They found average heat fluxes $F_H \approx 0.02 \rightarrow 0.1$ W m^{-2} by estimating F_H for each step. Although this form yields only small differences to (6), for the purposes of direct comparison we used (7) to find average heat fluxes from the ITP measurements to be $F_H = 0.22 \pm 0.10$ W m^{-2}. Heat fluxes through the present-day staircase appear to be about 3 or 4 times larger than they were in 1985, possibly a manifestation of the recent increased AW heat advection into the Canada Basin. It is worth noting, however, that heat fluxes supported by the present-day staircase are lower (only about twice as large as Padman and Dillon's estimates) in that part of the ITP survey region nearest the AIWEX measurements (Figures 1 and 7); that is, there exists the possibility that the differences are spatial rather than due to AW temperature increases over time. In any case, today's AW heat fluxes remain an order of magnitude less than recent estimates of vertical heat flux at the ocean surface [e.g., *Maykut and McPhee*, 1995; *Perovich and Elder*, 2002; *Krishfield and Perovich*, 2005; W. J. Shaw and T. Stanton, unpublished data, 2008], which range from a few W m^{-2} to around 40 W m^{-2}. That is, the double-diffusive AW heat flux is only a small fraction of the total ocean-to-ice heat flux. Turbulent mechanisms for AW heat transport (discussed in section 4) may contribute more. We note that most of the surface ocean heat influencing the sea ice derives from solar energy (see, for example, *Perovich and Elder* [2002], *McPhee et al.* [2003], and *Perovich et al.* [2007]); there is some evidence also that pycnocline upwelling of warmer Pacific-derived water below the surface mixed layer can increase ocean-to-ice heat fluxes locally [*McPhee et al.*, 2005].

3.4. Are Double-Diffusive Flux Laws Appropriate?

[14] The validity of the 4/3 flux laws may be verified by comparison to more direct heat flux estimates. If the interfaces between mixed layers were resolved, molecular heat transport through the high-gradient interfaces could be computed for comparison with estimates from the double-diffusive flux laws. In the absence of turbulent mixing, the conductive heat flux across interfaces can be estimated by $F_M = \rho c_p \kappa \partial\theta/\partial z$. The ITP permits the resolution of 25 cm thick interfaces at its nominal profiling speed and sample rate, while for typical $\delta\theta$, the interfaces would have to be less than half as thick for the molecular fluxes to be in agreement with our double-diffusive heat flux estimates. However, a microstructure profile taken in the ITP survey region that has better than 2 cm resolution in the vertical indicates diffusive interface thicknesses that are expected given heat fluxes computed in the previous section (Figure 8). The microstructure profile through the staircase indicates interface gradients $\partial\theta/\partial z = 0.36 \pm 0.09$ °C m^{-1}, to yield a molecular heat flux of $F_M \approx 0.2$ W m^{-2}, in agreement with the 4/3 flux-law estimates.

[15] It is of interest to calibrate 4/3 flux laws on the basis of field data. In particular, *Radko* [2007] proposes that evolution of a double-diffusive staircase can occur through merging events whereby interfaces across which the buoyancy difference is larger grow at the expense of interfaces with smaller buoyancy variation. He formulates a timescale (that depends on buoyancy fluxes) for merging based on a linear stability analysis of buoyancy conservation equations for a series of identical steps; the statistics of merger timescales can be used to calibrate 4/3 flux laws. Layer merging ceases when layer thickness reaches a critical value and the staircase equilibrates [*Radko*, 2005]. It seems unlikely that layer $\theta - S$ properties would group on discrete lines over basinwide lateral scales and in observations spanning several years if layers and interfaces were continuously merging and splitting (i.e., the Canada Basin staircase appears to be close to a stable equilibrium). Nevertheless, our preliminary inspection suggests there may be occasional merging and splitting in the double-diffusive staircase, and

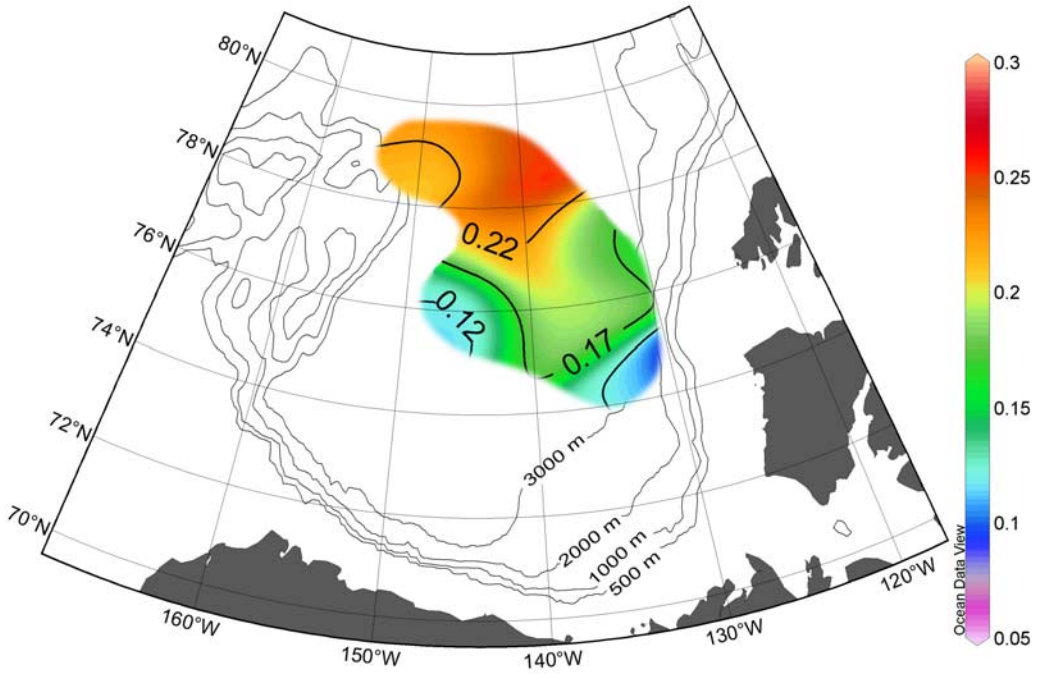

Figure 7. Map of heat flux (W m^{-2}) estimated by (6) averaged over the 200 m to 300 m deep thermohaline staircase from the ITP profiles.

future analysis may prove whether such events can be used to provide useful information for calibrating 4/3 flux laws.

4. Turbulent Mixing

[16] Although the persistence and coherence of the double-diffusive staircase point to double diffusion as the dominant mixing mechanism in the central basin thermocline, occasional disruptions to the staircase stratification indicate turbulent mixing. Here we use energy arguments to estimate the potential for turbulent mixing to drive higher heat fluxes. *Halle and Pinkel* [2003] measured downward internal wave energy fluxes beneath ice cover in the western Canada Basin (between December 1993 and January 1994, around 75°N, 150°W) to be between 0.02 mW m^{-2} and 0.15 mW m^{-2}, with the highest values during winter storm events. By assuming that all of this energy is dissipated in the thermocline, we can obtain an upper bound on a turbulent diffusivity there. This surface energy input would require a dissipation rate of kinetic energy ε of around 1×10^{-9} W kg^{-1} (dividing by the approximately 100 m thick thermocline, and the density of water). Following *Oakey* [1982], this corresponds to an effective turbulent vertical diffusivity of $K \approx \varepsilon/5\overline{N^2} \approx 5 \times 10^{-6}$ m^2 s^{-1}, where $\overline{N^2} = -g(\alpha\partial\overline{\theta}/\partial z - \beta\partial\overline{S}/\partial z) \approx 4 \times 10^{-5}$ s^{-1} is the buoyancy frequency based on the mean gradients of temperature and salinity over the thermocline. This K corresponds to an AW heat flux $F_H = K(\rho c_p \partial\overline{\theta}/\partial z) \approx 0.3$ W m^{-2}, about the same as double-diffusive heat flux estimates. Although more wind energy input may take place in seasonally ice-free areas, the large mixing rate required for AW heat to contribute significantly to the surface ocean heat budget, at least in the central Canada Basin, may not be energetically possible.

[17] CTD profiles from the Beaufort Gyre Observing System (www.whoi.edu/beaufortgyre/index.html) field program in the central and boundary regions of the Canada Basin indicate that the staircase stratification is disrupted or totally absent at the basin periphery (Figure 3b). While this may be due in part to $\overline{R_\rho}$ variability (e.g., higher $\overline{R_\rho}$ values to the south and east (Figure 3b) imply very weak double-diffusive fluxes there), staircase disruption is observed even in boundary regions where $\overline{R_\rho}$ values are lower. It is possible that there exist higher (turbulent) vertical heat fluxes at the basin boundaries [e.g., *Rainville and Winsor*, 2008]; addi-

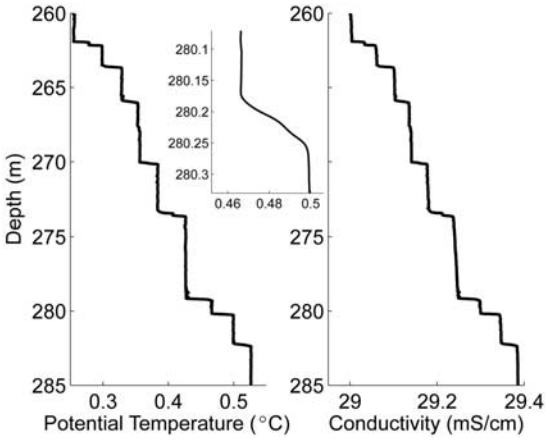

Figure 8. Potential temperature and conductivity profiles taken with a vertical microstructure profiler (Rockland Scientific International) during the pan-Arctic Beringia 2005 Expedition aboard the Swedish icebreaker *Oden* (26 August 2005, 78.5°N, 149.15°W). Variables were recorded at 512 Hz, and the instrument was lowered at 1 m s^{-1}.

tional microstructure measurements are needed to quantify dissipation rates.

[18] Heat might also escape the AW through enhanced turbulent mixing in the presence of eddies, and when warm AW upwells onto the continental shelves. *Toole et al.* [2006] observe a warm Atlantic Water eddy in the Canada Basin, around which the staircase is disrupted. Eddies are known to be regions of enhanced mixing; *Padman et al.* [1990] find evidence for higher dissipation rates within a shallower eddy in the Canada Basin. However, only a few eddies that appear to partially disrupt the staircase have been observed in the ITP survey region (Many shallower eddies have been observed immediately beneath the surface mixed layer [*Timmermans et al.*, 2008]. These do not impact the AW.); the net impact of AW eddies to the surface heat budget is uncertain. In contrast, AW upwelling events at the periphery of the Canada Basin (in canyons and along the continental margin) appear to be common [e.g., *Aagaard and Roach*, 1990; *Woodgate et al.*, 2005; *Nikolopoulos et al.*, 2008; R. S. Pickart and G. W. K. Moore, On the nature of upwelling storms in the western Arctic, submitted to Journal of Geophysical Research, 2008], and may provide meaningful contributions of AW heat to the surface.

5. Summary

[19] Ice-Tethered Profiler measurements confirm that Atlantic Water heat is transported vertically in the Canada Basin by double diffusion; the double-diffusive staircase is predominant at the top boundary of the AW throughout the central basin. Mixed layers in the staircase are shown to be laterally coherent for at least 800 km across the basin, with layer properties clustering along tightly bounded lines in $\theta - S$ space. The constant slopes of these lines may be explained in terms of a balance between along-layer advective divergence of temperature and salinity and vertical divergences of double-diffusive temperature and salt fluxes. The double-diffusive flux parameterization of *Kelley* [1990] yields heat fluxes between 0.05 and 0.3 W m^{-2}, in agreement with microstructure measurements. Vertical heat transport from the AW in the central Canada Basin likely provides only a small fraction of the total heat input to overlying waters, and it is possible that heat from the Atlantic Water escapes vertically primarily at boundary regions where there may be enhanced boundary mixing and upwelling.

[20] **Acknowledgments.** We are grateful to our colleagues from the Institute of Ocean Sciences, the Woods Hole Oceanographic Institution, and from the Japan Agency for Marine-Earth Science and Technology for collaborating on the BGOS and JWACS field programs, and the Canadian Coast Guard and the captains, officers, and crews of the CCGS *Louis S. St-Laurent* for icebreaker and helicopter support during the ITP deployments and CTD data collection. Special thanks to Andrey Proshutinsky, Eddy Carmack, Fiona McLaughlin, and Sarah Zimmermann. Initial development of the ITP concept was supported by the Cecil H. and Ida M. Green Technology Innovation Program. Funding for construction and deployment of the prototype ITPs was provided by the National Science Foundation Oceanographic Technology and Interdisciplinary Coordination (OTIC) Program and Office of Polar Programs (OPP) under grant OCE-0324233. Continued support for the ITP field program and data analysis has been provided by the OPP Arctic Sciences Section under awards ARC-0519899, ARC-0631951, ARC-0713837, and internal WHOI funding. Any opinions, findings, and conclusions or recommendations expressed in this publication are those of the authors and do not necessarily reflect the views of the National Science Foundation. The microstructure profile was taken during the Beringia 2005 field program, and we are grateful to Luc Rainville and the officers and crew of the icebreaker *Oden*. Finally, we would like to thank Breck Owens, George Veronis, and two anonymous reviewers for helpful comments.

References

Aagaard, K., and A. T. Roach (1990), Arctic Ocean–shelf exchange: Measurements in Barrow Canyon, *J. Geophys. Res.*, *95*, 18,163–18,175.

Halle, C., and R. Pinkel (2003), Internal wave variability in the Beaufort Sea during the winter of 1993/1994, *J. Geophys. Res.*, *108*(C7), 3210, doi:10.1029/2000JC000703.

Johnson, G. C., J. M. Toole, and N. G. Larson (2007), Sensor corrections for Sea-Bird SBE-41CP and SBE-41 CTDs, *J. Atmos. Oceanic Technol.*, *24*, 1117–1130.

Kelley, D. E. (1990), Fluxes through diffusive staircases: A new formulation, *J. Geophys. Res.*, *95*, 3365–3371.

Kelley, D. E., H. J. S. Fernando, A. E. Gargett, J. Tanny, and E. Özsoy (2003), The diffusive regime of double-diffusive convection, *Prog. Oceanogr.*, *56*, 461–481.

Krishfield, R., and D. Perovich (2005), Spatial and temporal variability of oceanic heat flux to the Arctic ice pack, *J. Geophys. Res.*, *110*, C07021, doi:10.1029/2004JC002293.

Krishfield, R., K. Doherty, D. Frye, T. Hammar, J. Kemp, D. Peters, A. Proshutinsky, J. Toole, and K. von der Heydt (2006), Design and operation of automated Ice-Tethered Profilers for real-time seawater observations in the polar oceans, *Tech. Rep. WHOI-06-11*, Woods Hole Oceanogr. Inst., Woods Hole, Mass.

Krishfield, R., J. Toole, A. Proshutinsky, and M.-L. Timmermans (2008), Automated Ice-Tethered Profilers for seawater observations under pack ice in all seasons, *J. Atmos. Oceanic Technol.*, *25*, 2091–2105, doi:10.1175/2008JTECHO587.1.

Marmorino, G. O., and D. R. Caldwell (1976), Heat and salt transport through a diffusive thermohaline interface, *Deep Sea Res. Oceanogr. Abstr.*, *23*, 59–67.

Maykut, G. A., and M. G. McPhee (1995), Solar heating of the Arctic mixed layer, *J. Geophys. Res.*, *100*, 24,691–24,703.

McDougall, T. (1987), Neutral surfaces, *J. Phys. Oceanogr.*, *17*, 1950–1964.

McDougall, T. (1991), Interfacial advection in the thermohaline staircase east of Barbados, *Deep Sea Res., Part A*, *38*, 357–370.

McLaughlin, F. A., E. C. Carmack, R. W. Macdonald, H. Melling, J. H. Swift, P. A. Wheeler, B. F. Sherr, and E. B. Sherr (2004), The joint roles of Pacific- and Atlantic-origin waters in the Canada Basin, 1997–1998, *Deep Sea Res., Part I*, *51*, 107–128.

McPhee, M. G., T. Kikuchi, J. H. Morison, and T. P. Stanton (2003), Ocean-to-ice heat flux at the North Pole environmental observatory, *Geophys. Res. Lett.*, *30*(24), 2274, doi:10.1029/2003GL018580.

McPhee, M. G., R. Kwok, R. Robins, and M. Coon (2005), Upwelling of Arctic pycnocline associated with shear motion of sea ice, *Geophys. Res. Lett.*, *32*, L10616, doi:10.1029/2004GL021819.

Morgan, P. (1994), SEAWATER: A library of MATLAB computational routines for the properties of seawater, *Rep. 222*, 29 pp., Commonw. Sci. and Ind. Res. Organ. Mar. Lab., Hobart, Tasmania.

Morison, J. H., K. Aagaard, and M. Steele (2000), Recent environmental changes in the Arctic: A review, *Arctic*, *53*, 4.

Neal, V. T., and S. Neshyba (1973), Microstructure anomalies in the Arctic Ocean, *J. Geophys Res.*, *78*, 2695–2701.

Neal, V. T., S. Neshyba, and W. Denner (1969), Thermal stratification in the Arctic Ocean, *Science*, *166*, 373–374.

Neshyba, S., V. T. Neal, and W. W. Denner (1971), Temperature and conductivity measurements under Ice Island T-3, *J. Geophys. Res.*, *76*, 8107–8120.

Neshyba, S., V. T. Neal, and W. W. Denner (1972), Spectra of internal waves: In-situ measurements in a multiple-layered structure, *J. Phys. Oceanogr.*, *2*, 91–95.

Nikolopoulos, A., R. S. Pickart, P. S. Fratantoni, K. Shimada, D. J. Torres, and E. P. Jones (2008), The western Arctic boundary current at 152°W: Structure, variability, and transport, *Deep Sea Res., Part II*, in press.

Oakey, N. S. (1982), Determination of the rate of dissipation of turbulent energy from simultaneous temperature and velocity shear microstructure measurements, *J. Phys. Oceanogr.*, *12*, 256–271.

Padman, L., and T. M. Dillon (1987), Vertical fluxes through the Beaufort Sea thermohaline staircase, *J. Geophys. Res.*, *92*, 799–806.

Padman, L., and T. J. Dillon (1988), On the horizontal extent of the Canada Basin thermohaline steps, *J. Phys. Oceanogr.*, *18*, 1458–1462.

Padman, L., and T. M. Dillon (1989), Thermal microstructure and internal waves in the Canada Basin diffusive staircase, *Deep Sea Res., Part A*, *36*, 531–542.

Padman, L., M. Levine, T. Dillon, J. Morison, and R. Pinkel (1990), Hydrography and microstructure of an Arctic cyclonic eddy, *J. Geophys. Res.*, *95*, 9411–9420.

Perkin, R. G., and E. L. Lewis (1984), Mixing in the West Spitsbergen Current, *J. Phys. Oceanogr.*, *14*, 1315–1325.

Perovich, D. K., and B. Elder (2002), Estimates of ocean heat flux during SHEBA, *Geophys. Res. Lett.*, *29*(9), 1344, doi:10.1029/2001GL014171.

Perovich, D. K., B. Light, H. Eicken, K. F. Jones, K. Runciman, and S. V. Nghiem (2007), Increasing solar heating of the Arctic Ocean and adjacent seas, 1979–2005: Attribution and role in the ice-albedo feedback, *Geophys. Res. Lett.*, *34*, L19505, doi:10.1029/2007GL031480.

Radko, T. (2005), What determines the thickness of layers in a thermohaline staircase?, *J. Fluid Mech.*, *523*, 79–98.

Radko, T. (2007), Mechanics of merging events for a series of layers in a stratified turbulent fluid, *J. Fluid Mech.*, *577*, 251–273.

Rainville, L., and P. Winsor (2008), Mixing across the Arctic Ocean: Microstructure observations during the Beringia 2005 Expedition, *Geophys. Res. Lett.*, *35*, L08606, doi:10.1029/2008GL033532.

Rudels, B., P. Jones, U. Schauer, and P. Eriksson (2004), Atlantic sources of the Arctic Ocean surface and halocline waters, *Polar Res.*, *23*(2), 181–208.

Schmitt, R. W. (1988), Mixing in a thermohaline staircase, in *Small-Scale Turbulence and Mixing in the Ocean*, edited by J. Nihoul and B. Jamart, *Elsevier Oceanogr. Ser.*, *46*, 435–452.

Schmitt, R. W., H. Perkins, J. D. Boyd, and M. C. Stalcup (1987), C-SALT: An investigation of the thermohaline staircase in the western tropical North Atlantic, *Deep Sea Res., Part A*, *34*, 1697–1704.

Serreze, M. C., J. E. Walsh, F. S. Chapin III, T. Osterkamp, M. Dyurgerov, V. Romanovsky, W. C. Oechel, J. Morison, T. Zhang, and R. G. Barry (2000), Observational evidence of recent change in the northern high latitude environment, *Clim. Change*, *46*, 159–207.

Shimada, K., F. McLaughlin, E. Carmack, A. Proshutinsky, S. Nishino, and M. Itoh (2004), Penetration of the 1990s warm temperature anomaly of Atlantic Water in the Canada Basin, *Geophys. Res. Lett.*, *31*, L20301, doi:10.1029/2004GL020860.

Timmermans, M.-L., J. Toole, A. Proshutinsky, R. Krishfield, and A. Plueddemann (2008), Eddies in the Canada Basin, Arctic Ocean, observed from Ice-Tethered Profilers, *J. Phys. Oceanogr.*, *38*, 133–145.

Toole, J., et al. (2006), Ice-Tethered Profilers sample the upper Arctic Ocean, *Eos Trans. AGU*, *87*(41), doi:10.1029/2006EO410003.

Turner, J. S. (1968), The behavior of a stable salinity gradient heated from below, *J. Fluid Mech.*, *33*, 183–200.

Woodgate, R. A., K. Aagaard, J. H. Swift, K. K. Falkner, and W. M. Smethie (2005), Pacific ventilation of the Arctic Ocean's lower halocline by upwelling and diapycnal mixing over the continental margin, *Geophys. Res. Lett.*, *32*, L18609, doi:10.1029/2005GL023999.

R. Krishfield, M.-L. Timmermans, J. Toole, and P. Winsor, Woods Hole Oceanographic Institution, 266 Woods Hole Road, Woods Hole, MA 02543, USA. (mtimmermans@whoi.edu)